Journal of Cell Science 105, 541-550 (1993)
Printed in Great Britain © The Company of Biologists Limited 1993

Visualization of replication sites in unfixed human cells

A. Bassim Hassan and Peter R. Cook*

Sir William Dunn School of Pathology, University of Oxford, South Parks Road, Oxford OX1 3RE, UK

*Author for correspondence

SUMMARY

Sites of DNA replication in nuclei are focally concentrated, suggesting that an underlying structure organizes the activity of many polymerases. As fixation could induce aggregation into foci, we examined the distribution of replication sites in unfixed nuclei. HeLa cells were encapsulated in agarose microbeads, permeabilized in a 'physiological' buffer, their DNA polymerizing activity characterized, and replication sites directly labelled by incubation with fluorochrome-dUTP conjugates. Using conventional and digital fluorescence microscopy, 80-250 foci were seen in these unfixed cells. These foci are unlikely to be formed by the aggregation of separate polymerases as most replication activity found in vivo is retained throughout these procedures. Although commonly used fixation methods collapsed or dispersed their periphery, the central core was very stable. Foci remained when ~90% chromatin was removed, suggesting they were attached to an underlying structure.

Key words: replication foci, DNA polymerase, nucleoskeleton, dTTP analogues, fixation

INTRODUCTION

A variety of evidence suggests that active DNA polymerases are bound to an underlying structure in the eukaryotic nucleus, with replication occurring as DNA is reeled through an attached complex (Laskey et al., 1989; Jackson, 1990; Cook, 1991). For example, Berezney and Coffey (1975) showed that nascent DNA was tightly associated with a residual nuclear 'matrix' and this observation led to many subsequent studies (e.g. see Pardoll et al., 1980; McCready et al., 1980; Jackson, 1991). But such results have been dogged by the criticism that nascent DNA and associated polymerases, being very sticky, had aggregated artifactually during extraction in the high salt concentrations used for isolation (e.g. see Martelli et al., 1990). Any role for a matrix - and even its existence in vivo - remains controversial (Cook, 1988).

A second set of observations provides additional, albeit circumstantial, evidence for attached polymerases. If polymerases are freely diffusible, we might expect synthetic sites to be spread throughout nuclei, reflecting the template concentration. However, sites are not diffusely scattered but focally concentrated, with many polymerases within a focus firing co-ordinately. For example, Nakamura et al. (1986) labelled rat cells in S-phase with bromodeoxyuridine and then visualized incorporation sites using fluorescence-labelled antibodies directed against the analogue; ~130 discrete foci, each of which must contain ~20 replication units, were seen. Cells at different stages during S-phase give characteristic patterns (Nakamura et al., 1986; see also Nakayasu and Berezney, 1989). These studies have been widely confirmed (e.g. see Fox et al., 1991; Kill et al., 1991; O'Keefe et al., 1992) and particles containing the requisite number of polymerases can be extracted from nuclei (Tubo and Berezney, 1987).

Similar foci are also seen using biotin-dUTP and FITC-streptavidin after incubating de-membranated sperm in extracts of frogs' eggs (Blow and Laskey, 1986, 1988; Hutchison et al., 1987; Mills et al., 1989). A membrane reforms and DNA is replicated efficiently in 100-300 foci distributed throughout the nuclei. Since replication occurs so quickly, each focus must contain 300-1000 replication forks; it is difficult to see how so many unattached polymerases could act so co-ordinately and so focally without being integrated in space by some structure.

However, it remains possible that the fixation used for immunofluorescence artifactually aggregates dispersed polymerization sites into foci. For example, sites of incorporated bromodeoxyuridine can be visualized after extracting cells with strong acids to expose the incorporated analogue to antibodies (Nakamura et al., 1986; Dolbeare and Gray, 1988; Fox et al., 1991; O'Keefe et al., 1992). Treatments commonly used to fix tissue-culture cells also reorganize one of the components of the replicating complex, proliferating cell nuclear antigen (PCNA; Bravo and Macdonald-Bravo, 1987), an snRNP (Carmo-Fonseca et al., 1991) and other proteins (Melan and Sluder, 1992). Therefore we developed methods for labelling replication sites in unfixed cells. We first characterized the polymerizing activity in our system, established what the 'native' pattern of sites was, and then investigated the effects of commonly-used fixation procedures on the pattern.

Our approach is based on the use of cells encapsulated in agarose microbeads (r = ~25 μm; Jackson et al., 1988); the encapsulating agarose protects fragile cell remnants during manipulation (e.g. pelleting). After lysing cell membranes, incubation with the appropriately labelled triphosphates and thorough washing, sites of incorporation can be viewed in unfixed cells. As the permeabilized cells retain essentially all the replicational activity of the living cell, and as 'physiological' conditions are used throughout, it seems unlikely that the focal sites of incorporation seen are aggregation artifacts.

MATERIALS AND METHODS

Cell culture and synchronization

Suspension cultures of HeLa cells were grown in minimal essential medium supplemented with 10% foetal calf serum. Prior to replication assays, cells were grown in [*methyl*-^{3}H]thymidine (0.05 μCi/ml; ~60 Ci/mmol) for 18-24 hours to label their DNA uniformly, and allow corrections for slight variations in cell numbers. Cells were synchronized using thymidine and nitrous oxide (Jackson and Cook, 1986b): cells were first blocked in S-phase (2.5 mM thymidine, 22 h), washed thoroughly and regrown for 4 h in fresh medium. Then, >95% were induced to arrest at mitosis using nitrous oxide at high pressure (8 h), and regrown in fresh medium. The first cells enter S-phase 5 h later. Early, mid and late S-phase cells were taken 8, 11 and 14 h post-mitosis respectively.

Encapsulation and lysis

Cells were washed 3× in PBS and encapsulated (10^6-10^7 cells/ml) in 0.5% agarose (Jackson et al., 1988). Encapsulated cells were incubated with streptolysin O (1000 i.u./ml per 10^6 cells, 30 min, 4°C; Sigma) in an equal volume of ice-cold PBS, washed with 10 vols ice-cold PBS to remove unbound streptolysin O and then with 10 vols ice-cold 'physiological' buffer (PB). PB contains 22 mM Na^+, 130 mM K^+, 1 mM Mg^{2+}, <0.3 μM free Ca^{2+}, 132 mM Cl^-, 11 mM phosphate, 1 mM ATP (grade I; Sigma), 1 mM dithiothreitol and 0.1 mM phenylmethylsulphonyl fluoride (PMSF). Beads were resuspended in an equal volume of PB and permeabilized (35°C, 2 min). Permeabilization (>95% lysis) of the plasma membrane was routinely monitored by trypan blue; the nuclear membrane remained intact as FITC-IgG (1:500; Amersham) was excluded from nuclei (Leno et al., 1992). Encapsulated cells were also permeabilized (10 min; 4˚C) with 0.5% Triton X-100 in PB, and washed 4× with 10 vols PB.

Replication assays

Encapsulated cells were pre-incubated (35˚C, 2 min) and reactions started by adding triphosphates (Pharmacia-LKB); final concentrations were generally 0.1 mM CTP, UTP and GTP, 0.25 mM dCTP, dATP and dGTP, 0.2 mM $MgCl_2$ with either (i) [^{32}P]dTTP (~3000 Ci/mmol, 10-20 μCi/ml; Amersham) plus unlabelled dTTP added to the concentration indicated or (ii) analogues of dTTP. In some cases [^{32}P]dGTP (~3000 Ci/mmol, 10-20 μCi/ml; Amersham) was used as radiolabel; then unlabelled dGTP was added (to the concentration indicated) and also 0.25 mM dTTP. Variations from standard conditions are given in the Fig. legends. Reactions using radiolabel were stopped by removing samples at various times and adding an equal volume of 2% SDS; samples were incubated (2 h, 37˚C) and ^{32}P incorporation into acid-insoluble material was measured by scintillation counting (Jackson and Cook, 1986b). Samples for light microscopy were stopped by washing in 10 vols ice-cold PB. dTTP analogues used were biotin-11-dUTP (Sigma), biotin-16-dUTP (Boehringer), biotin-21-dUTP (Clontech), fluorescein-12-dUTP (Boehringer), resorufin-10-dUTP (Boehringer) and hydroxycoumarin-6-dUTP (Boehringer). Aphidicolin (Sigma), VM 26 (Bristol Myers), camptothecin (Sigma), hydroxyurea (Sigma), ionomycin (Sigma), A23187 (Sigma) and wheat germ agglutinin (Sigma) were preincubated (4˚C, 2 min) before the usual preincubation. Brefeldin A (Sigma) was added to cells in culture 30 min prior to encapsulation.

Digestion and electrolution

After incorporation of dTTP analogues, nuclear membranes were permeabilized with 0.5% Triton X-100 (10 vol, 4˚C, 2 × 10 min). Beads were then incubated (33˚C, 20 min) with *Eco*RI (2500 i.u./ml) and *Hae*III (500 i.u./ml) in PB and subjected to electrophoresis (0.8% agarose, 4 V/cm, 4 h; Jackson et al., 1988) in modified PB (130 mM KCl replaced with 65 mM KCl and 65 mM potassium acetate to reduce pH drift) supplemented with fresh PMSF (>0.1 mM). Generally 90% ^{3}H (i.e. chromatin) eluted from beads (Jackson et al., 1990; Hozák et al., 1993).

Fluorescence microscopy

Generally, samples were not fixed prior to fluorescence microscopy. After incubation with fluorochrome-conjugated triphosphates, beads were washed 1× in ice-cold PB plus 0.02% Tween-20 to remove free fluorochrome, and immediately visualized after mounting under coverslips in PB ± 4′,6′-diamidino-2-phenylindole (DAPI, 0.1 μg/ml; Boehringer). After incubation with biotin-dUTP, nuclei were permeabilized with 0.5% Triton X-100 in PB (10 min at 4˚C, followed by 4 washes with 10 vols PB) and beads (100 μl packed vol.) incubated with streptavidin-FITC (0.5 pg/ml, 16 h, 4˚C; Sigma) in PB plus 0.02% Tween-20 (2 ml); beads were then washed (5×, 100 vols) in PB and mounted under coverslips. For Fig. 8, nuclear membranes were permeabilized as above and beads treated (4˚C, 15 min) with different fixation procedures; then 100 μl samples were washed (5×, 100 vols) in PB and mounted under coverslips in PB + DAPI (0.1 μg/ml) and Mowiol (Hoechst) before microscopy.

Conventional photographs were taken using a Zeiss Axiophot microscope (standard filter sets) fitted with an Optivar lens (×1.6) using Kodak EES colour or T-max black and white film, both push-processed to ASA 1600. Typical exposures were 20-30 s and 2-5 s for fluorescent tracers and DAPI, respectively. Digital images were also captured using a Hamamatsu charge-coupled device (CCD, C4742, 1000×1018 pixel, −40˚C, Peltier-cooled) attached to the Axiophot (Optivar lenses ×1.25 to ×1.6, ×100 oil-immersion lens, NA 1.3). Images from several focal planes (n=8-10; z step, 0.5 μm) were deconvolved to remove out-of-focus flare using Micro-Tome Mac software (nearest-neighbour deblurring algorithm; Vaytec Inc) run on a modified Macintosh Quadra computer. The appropriate point-spread function parameters were adjusted before deconvolution of median-filtered images.

An MRC 600 laser scanning confocal microscope (Bio-Rad) fitted with an argon-ion laser (λ=514) attached to Nikon Diaphot inverted microscope (×60 oil-immersion objective, NA 1.4) was also used to detect unfixed fluorescein and resorufin-fluorescent foci (Kallman filtered images; ×2.5 zoom; z step, 0.7 μm).

RESULTS

Lysing the nuclear membrane reduces replication efficiency

After permeabilizing cell membranes using complement and the appropriate antibodies, encapsulated HeLa cells

elongate nascent DNA chains at the in vivo rate when provided with optimal concentrations of triphosphates (Jackson et al., 1988). (Note that we assay activities of a polymerase that is halted at lysis and then continues synthesis in vitro without reinitiation (Jackson and Cook, 1986a,b,c).) Lysing both cell and nuclear membranes with Triton X-100 reduces the synthetic rate, presumably because lysis of the nuclear membrane releases some factor(s) that enhances efficiency (Jackson et al., 1988).

As complement-mediated lysis proved to be variable, we now routinely use streptolysin O. At 4˚C this bacterial protein binds to cholesterol in membranes and, on raising the temperature to 35˚C, it rapidly assembles into 35 nm pores (Ahnert-Higler et al., 1989). Rapid lysis is advantageous because polymerizing activity is thermolabile (see below). [^{32}P]dGTP is then incorporated into acid-insoluble material for up to 2 h (Fig. 1; SO); initial rates after lysis with Triton X-100 are about four-fold less (Fig. 1; T). Similar results were obtained with labelled dTTP, dATP or dCTP rather than [^{32}P]dGTP (not shown). Under the conditions in Fig. 1, where 10 μM dGTP limits synthesis, and assuming ~5500 replication forks are active in each nucleus at any one time (see Discussion), ~3 kb and ~500 bp are replicated at each fork in 2 h by streptolysin-O- and Triton-X-100-lysed cells, respectively. Aphidicolin (5 μg/ml), an inhibitor of DNA polymerase α (Krokan et al., 1981) reduced incorporation, but did not eliminate it (Fig. 1, SO + Aphi and T + Aphi; Table 1); residual activity probably results from inefficient competitive inhibition with the 250 μM dCTP pool. Proteins in nuclei prepared by conventional procedures, but not in our preparation, are prone to aggregate at 37˚C; even so, we routinely conduct replication assays at 35˚C to eliminate any possibility of such aggregation (for a discussion, see Jackson et al., 1988).

The complete replication mixture contains nucleotide triphosphates (NTPs) necessary for synthesis of RNA primers, so some of these may be incorporated into DNA after reduction by ribonucleotide reductase. Therefore we investigated the effect of omitting different triphosphates from the reaction (Table 1). Omission of unlabelled deoxynucleotide triphosphates (dNTPs) reduced incorporation to 25% (but not to the 0% expected if they were the sole precursors) and omission of three NTPs roughly halved the rate. However, hydroxyurea, which inhibits ribonucleotide reductase, only slightly reduced incorporation. These results are most simply explained if (i) dNTPs are used if present, (ii) there is slight incorporation of NTPs after reduction and (iii) dNTPs present as residual pools or contaminants in the NTPs become significant precursors in the absence of added dNTPs. Incorporation is also insensitive to inhibitors of topoisomerases I and II (i.e. camptothecin, VM 26), even over a period of 30 min, when substantial amounts of DNA are replicated.

Activity in cells lysed with either streptolysin O or Triton X-100 is thermo-labile; incorporation falls as preincubation at 35˚C is increased from 0-15 min (Fig. 2; SO and T at 0, 5, 15 min). Similar results were obtained previously after lysis with Triton X-100 (Jackson and Cook, 1986c). Addition of 0.5% Triton X-100 after 5 min to streptolysin-O-lysed cells reduced activity (Fig. 2, arrows and SO/T); again this is compatible with release of some factor(s) that enhances efficiency. As expected, addition of Triton X-100 after 5 min to Triton-X-100-lysed cells had no effect (not shown).

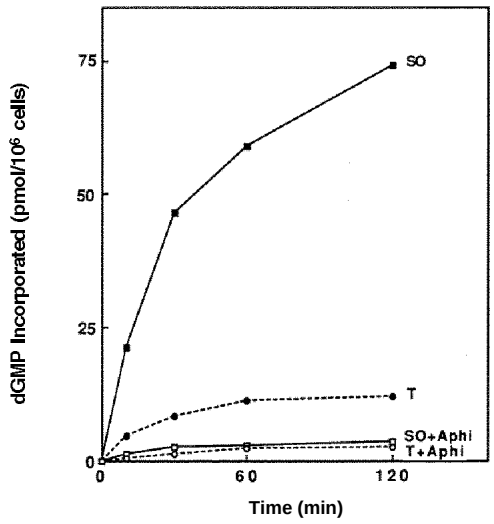

Fig. 1. Rates of incorporation of 10 μM [^{32}P]dGTP into acid-insoluble material by encapsulated and unsynchronized cells lysed either with streptolysin O (SO) or Triton X-100 (T), in the presence or absence of aphidicolin (Aphi, 5 μg/ml).

Effects of ionic environment on replication

It was possible that an intact nuclear membrane might buffer activity within streptolysin-O-lysed cells from changes in the environment. However, altering the pH of the physiological buffer had comparable effects on streptolysin-O- and Triton-X-100-lysed cells (Fig. 3); no differential effects were detected by varying the external Ca^{2+} concentration between 0.2 μM-1000 μM or by the addition of the ionophores, ionomycin and A23187 (5 μM; not shown). Disruption of the endoplasmic reticulum by brefeldin A also had no significant effect, nor did blocking

Table 1. The effect of various treatments on replication rates after lysing cells with streptolysin O

Treatment	Relative efficiency (%) 15 s - 5 min	15 s - 30 min
Complete mixture	100	100
−unlabelled dNTPs	25	nd
−CTP, GTP and UTP	54	nd
−all unlabelled triphosphates	3	nd
+HU (5 mM)	89	87
+HU (5 mM)−unlabelled dNTPs	20	nd
+HU (5 mM),−CTP, GTP and UTP	53	nd
+calcium (0.2 μM)	97	84
+calcium (1000 μM)	20	21
+brefeldin A (5 μg/ml)	98	83
+aphidicolin (5 μg/ml)	2	4
+VM26 (tenoposide; 100 μg/ml)	92	92
+camptothecin (10 μg/ml)	82	84
+wheat germ agglutinin (0.1 mg/ml)	97	90

Rates were measured between 15 s and 5 min or 30 min using 2.5 μM [^{32}P]dTTP and expressed relative to an untreated control. HU, hydroxyurea; nd, not determined.

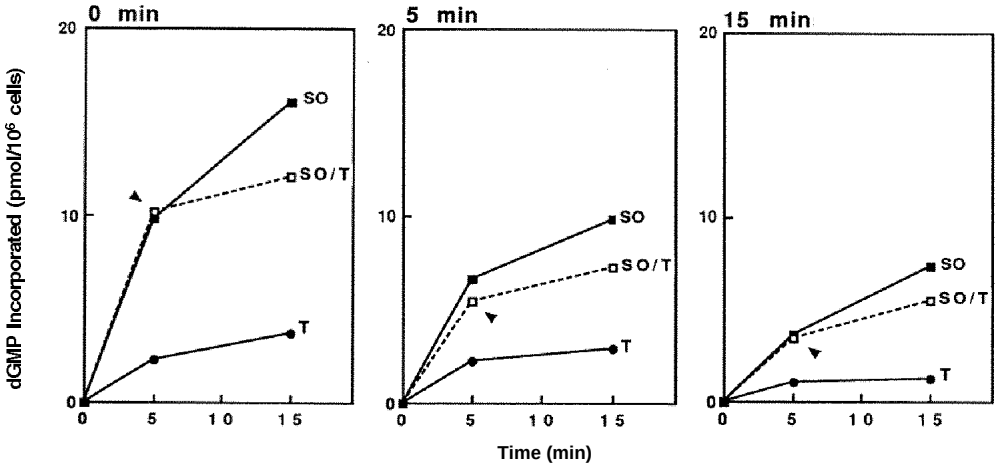

Fig. 2. The effect of preincubation (0, 5, and 15 min) at 35°C on incorporation of [^{32}P]dTTP (10 μM) by cells permeabilized with streptolysin O (SO) or Triton X-100 (T). Triton X-100 (0.5%) was also added 5 min after initiation by streptolysin-O-lysed cells (arrows, SO/T).

nuclear pores with wheat germ agglutinin (Table 1; Finlay et al., 1987).

Kinetics of DNA synthesis

The use of different permeabilization procedures and triphosphate concentrations has given values from 1-85 μM for the K_m of triphosphates during replication by permeabilized cells (e.g. see Miller et al., 1978; Krokan et al., 1981; Reddy and Pardee, 1982; Jackson and Cook, 1986b; Dresler et al., 1988). Therefore we varied the concentrations of all four dNTPs, or just dTTP, and monitored rates (Fig. 4A); NTPs were included in all reactions. Rates after lysis with streptolysin O were 2-4× higher than those after lysis with Triton X-100, depending on the dNTP concentration. Triphosphate concentrations >20 μM gave initial rates equivalent to, or greater than, those found in vivo.

A Lineweaver-Burk plot of the results of 4 experiments like those in Fig. 4A is non-linear, giving 2 (apparent) K_m values (Fig. 4B; arrows on abscissa give values of 0.9 and 19 μM). (The physiological concentration of dNTPs is approximately micromolar; for a review, see Reichard (1988). Rates after lysis with streptolysin O are higher than after lysis with Triton X-100, but K_m values are similar. Removing CTP, GTP and UTP produces similar double-reciprocal plots and K_m values, although the overall efficiency is roughly halved (not shown).

Incorporation of dTTP analogues

Various analogues are available that permit subsequent visualization of their sites of incorporation by fluorescence microscopy. Replacing 2.5 μM dTTP with such analogues reduced rates; biotin-11-dUTP was incorporated the most efficiently of those tested (Table 2). Biotin-16-dUTP and biotin-21-dUTP were incorporated at 17% and 16% of the rate of dTTP, respectively (not shown).

Visualization of sites of replication in unfixed cells

Although these analogues are incorporated less efficiently than dTTP, rates are still sufficient to allow subsequent visualization. For example, encapsulated cells were permeabilized with streptolysin O and incubated for 2.5 min with biotin-11-dUTP; incorporation sites were then labelled with streptavidin-FITC. Fig. 5A illustrates a typical, unfixed, cell; faint fluorescent foci are visible. After incubation for 60 min, discrete foci become clearly visible (Fig. 5B) which do not coincide either with local concentrations of DNA (detected by staining the same cell with 4′,6′-diamidino-2-phenylindole, DAPI; Fig. 5C) or with phase-dense vesicles (Fig. 5D). As labelling intensities of cells within a bead varied ~4-fold, typical examples are given below. Unlike cells growing on coverslips, where nuclei are flattened, many foci in our round nuclei lie above or below the focal plane, generating an out-of-focus 'flare'; this makes visualization of individual foci difficult, unless they are in focus at the nuclear periphery.

Incubation with fluorescein-12-dUTP allows an even more immediate visualization of replication sites after washing away unincorporated label. Although little fluorescence due to incorporated analogue is visible to the eye after incubation for 2.5 min (Fig. 5E), fluorescent foci are

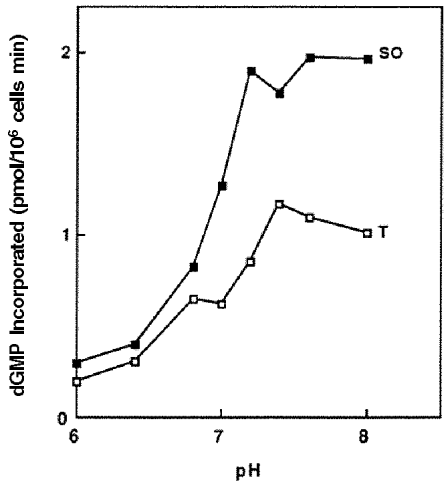

Fig. 3. The effect of pH on replication rate (measured between 15 s and 5 min using 10 μM [^{32}P]dTTP). Unsynchronized cells were lysed with streptolysin O (SO) or Triton X-100 (T) in PB adjusted to the appropriate pH: all subsequent washes and incubations were at the same pH. The final step in the preparation of PB usually involves addition of ATP to give a pH of 7.4; buffers with pH >7.4 were prepared by adding less ATP, and those with pH <7.4 by titration with HCl.

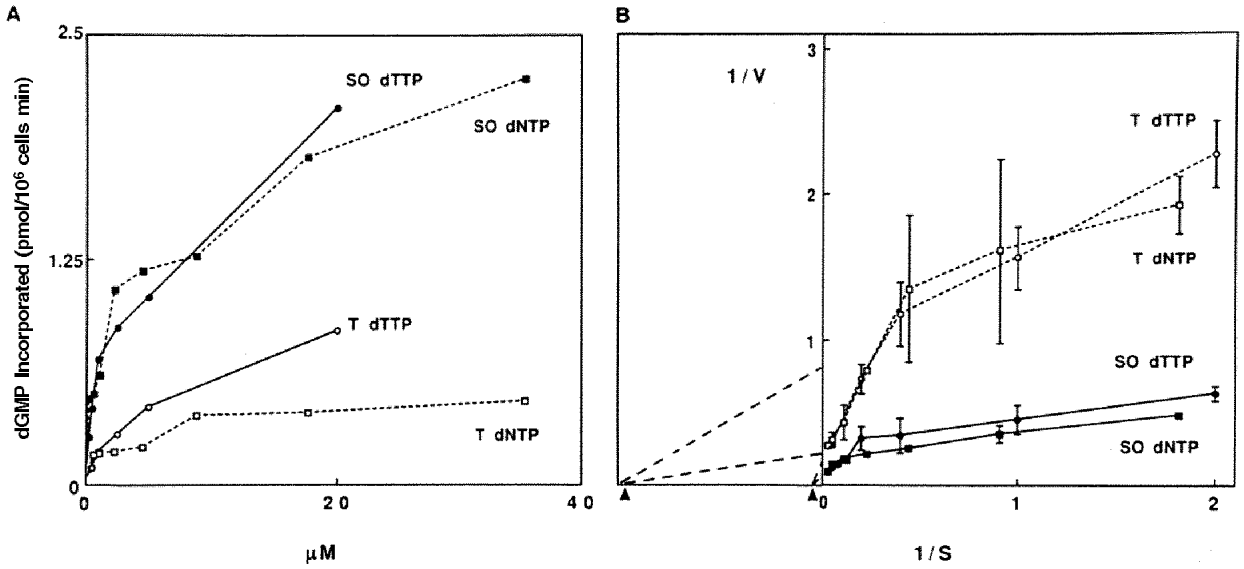

Fig. 4. The dependence of the rate of incorporation of [^{32}P]dTTP on triphosphate concentration. Concentrations of either dTTP, or all four dNTPs, were varied. Unsynchronized cells were permeabilized with streptolysin (SO) or Triton X-100 (T) and initial rates of incorporation determined (measured between 15 s and 5 min). The NTP concentration was held constant at 100 μM. (A) One typical example. (B) Double-reciprocal plot of means (±2 s.d.) of 4 experiments as in (A). The non-linear plots give similar K_m values for both streptolysin and Triton-X-100-lysed cells (arrows; K_m of 0.9 and 19 μM).

clearly visible after 60 min (Fig. 5F). Again, foci do not coincide with local concentrations of DNA (Fig. 5G) or with phase-dense vesicles (Fig. 5H). Similar, but fainter, foci were seen in cells lysed with Triton X-100 (not shown). Omission of three triphosphates (but inclusion of fluorescein-12-dUTP) eliminates labelling (Fig. 5I), as does incubation with aphidicolin (Hozák et al., 1993).

Although a 5 min incubation with fluorescein-12-dUTP gave no foci visible by conventional microscopy (not shown), they are clearly visible using a sensitive CCD camera (Fig. 6B). As red light is detected with even greater sensitivity than green, (red) foci can be seen after incubation with resorufin-10-dUTP for only 2.5 min (Fig. 6A). Digitized images can be easily distorted (e.g. by background subtraction and grey-scale manipulation) so primary images (i.e. median filtered and linearly contrast-extended to fill the 256 pixel grey-scale) are presented in Fig. 6A,B. Therefore they are views of whole cells against a 'real' background, including out-of-focus flare, and so are roughly comparable to those obtained by conventional photography.

The three-dimensional distribution of unfixed foci

Out-of-focus flare can be removed by applying a 'deblurring' algorithm to information from serial sections. Unsynchronized cells were permeabilized, incubated with resorufin-10-dUTP for 60 min and then optical slices were taken at 0.5 μm intervals through a nucleus with an early S-phase pattern; Fig. 6C and D show typical raw and deblurred images of one central section. These unfixed foci had diameters of 0.2-0.5 μm; many were clustered or arrayed in chains and were larger than those detected at 2.5 min (Fig. 6A), giving the impression that foci grow and so coalesce with time.

A confocal laser scanning microscope ('confocal' micro-

Table 2. The effect of dTTP analogues on replication rates by cells lysed with streptolysin O or Triton X-100

Permeabilizing agent	dTTP or analogue	dGMP incorporated (pmol/10^6 cells per min)	Relative rate
Streptolysin O	dTTP	0.93	1.0
	Biotin-11-dUTP	0.24	0.26
	Fluorescein-12-dUTP	0.17	0.18
	Resorufin-10-dUTP	0.16	0.17
	Hydroxycoumarin-6-dUTP	0.18	0.19
Triton X-100	dTTP	0.2	0.21
	Biotin-11-dUTP	0.07	0.07
	Fluorescein-12-dUTP	0.06	0.06
	Resorufin-10-dUTP	0.04	0.05
	Hydroxycoumarin-6-dUTP	0.06	0.06

Rates (measured between 15 s and 5 min; averages of 4 experiments) are expressed relative to the rate given by cells lysed with streptolysin O using dTTP; this was 40% of the rate in vivo (calculated assuming 8 pg DNA/nucleus is replicated in 22 h). Reactions contained 2.5 μM [^{32}P]dGTP, 250 μM dATP and dCTP, plus 20 μM dTTP or its analogues.

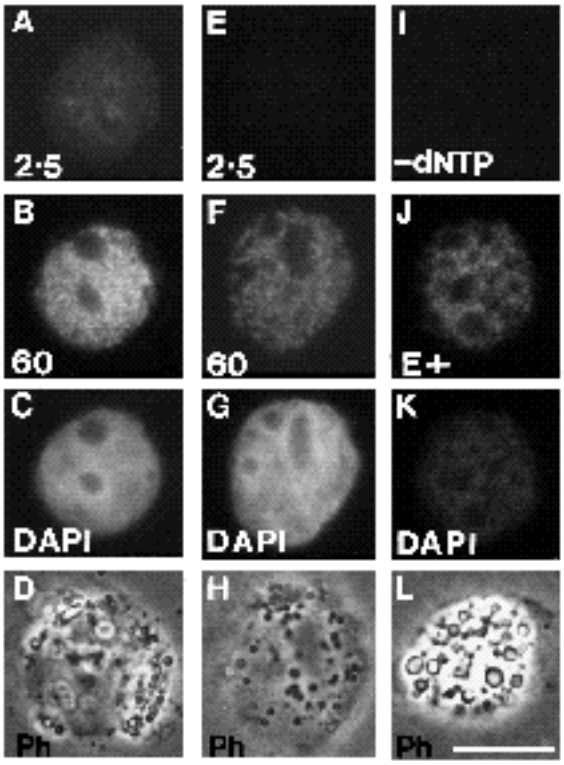

Fig. 5. Photomicrographs of replication sites in unfixed cells. Unsynchronized cells were permeabilized with streptolysin, incubated for different times with different analogues (10 μM) and incorporation sites viewed by conventional fluorescence microscopy. Cells were not fixed. Bar, 5 μm. (A) 2.5 min incubation with biotin-11-dUTP, followed by treatment with streptavidin-FITC. (B) As (A), 60 min incorporation. (C) Same cell as in (B), stained with DAPI. (D) Same cell as in (B), viewed under phase contrast (Ph). (E) 2.5 min incubation with fluorescein-12-dUTP; labelling cannot be detected. (F) 60 min incubation with fluorescein-12-dUTP. (G) Same cell as in (F), stained with DAPI. (H) Same cell as in (F), viewed under phase contrast. (I) 60 min incubation with fluorescein-12-dUTP but without other dNTPs. (J) 60 min incubation with fluorescein-12-dUTP, then ~90% chromatin was removed by nuclease digestion and electrophoresis (E+). (K) Same cell as in (J), stained with DAPI; the same exposure was used for (G) and (K). (L) Same cell as in (J), viewed with phase contrast (Ph).

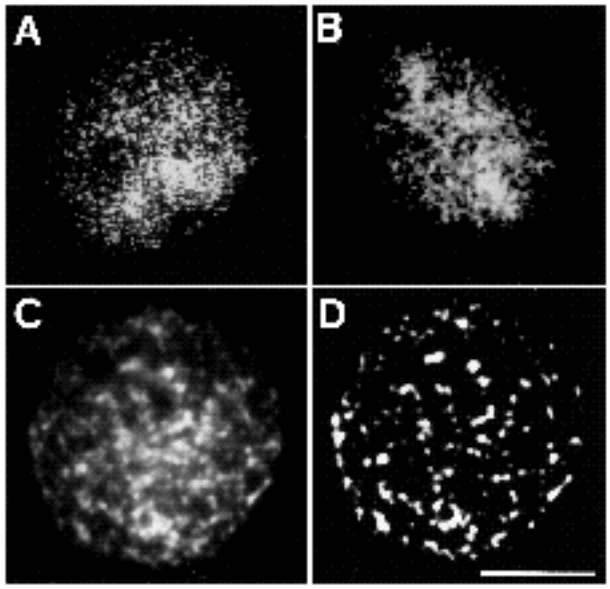

Fig. 6. Replication foci in unfixed and unsynchronized cells viewed using a CCD camera; all cells have the early S-phase pattern. (A,B) Cells were permeabilized, incubated with (A) 50 μM resorufin-10-dUTP for 2.5 min or (B) 50 μM fluorescein-12-dUTP for 5 min. Raw images of foci, which were barely visible to the naked eye by conventional microscopy, were captured by a CCD camera set at one third the maximum gain and minimally processed. (C) An example of one raw image from a series taken at 0.5 μm intervals through a typical nucleus after incubation with 10 μM resorufin-10-dUTP for 60 min. The image was captured using a single 2 s exposure with zero gain and then processed minimally; no other background was subtracted, nor were several exposures integrated over time or space. (D) The image in (C) after removal of out-of-focus flare using a nearest-neighbour deblurring algorithm. There were 203 foci in the whole of this larger-than-average nucleus (*d*, 11 μm; contiguous foci in adjacent sections in the series were counted as one). Bar, 5 μm.

scope) allows direct optical removal of out-of-focus flare. Synchronized cells from early, mid and late S-phase were encapsulated, permeabilized with streptolysin O and incubated with fluorescein-12-dUTP for 60 min. Then optical slices were taken at 0.7 μm intervals through typical nuclei; in Fig. 7, six central slices are shown on the right and a maximum projection of all the slices are shown on the left. Discrete foci are visible in cells from the different stages and each stage has a typical pattern, categorized as type I, II, or III (Nakamura et al., 1986; Nakayasu and Berezney, 1989; Kill et al., 1991). In early S-phase, foci are uniformly distributed throughout nuclei; they often touch each other, unlike the more discrete foci seen after fixation (see below). By mid S-phase they become clustered under the nuclear membrane and around nucleoli; later they form bright irregular crescents. There are typically 80-250 in these aneuploid cells (Fig. 7). If ~5500 replication forks are active at any one time, each focus must contain ~40 replication forks.

The effects of fixation on the structure of foci

We next investigated how fixation affected focus morphology (Fig. 8). Permeabilized cells were incubated with fluorescein-12-dUTP for 60 min, fixed in various ways, washed thoroughly, and nuclei with early S-phase patterns photographed using conventional microscopy; they should be compared with the unfixed control illustrated in Fig. 8O.

Paraformaldehyde best preserved the pattern found in unfixed cells (Fig. 8A); foci had similar sizes and intensities. After treatment with several fixation or 'stabilization' procedures (i.e. methanol, copper sulphate or trichloroacetic acid), foci become more intense and punctate (Fig. 8B,D,F). When living cells are incubated with bromodeoxyuridine, sites of incorporation are usually visualized after extraction with hydrochloric acid; perhaps surprisingly, such treatment preserves the structure of foci even though nuclear structure is disrupted, as evidenced by DAPI staining (Fig. 8C). Trichloroacetic acid (Fig. 8F) and, to a lesser extent, EGS

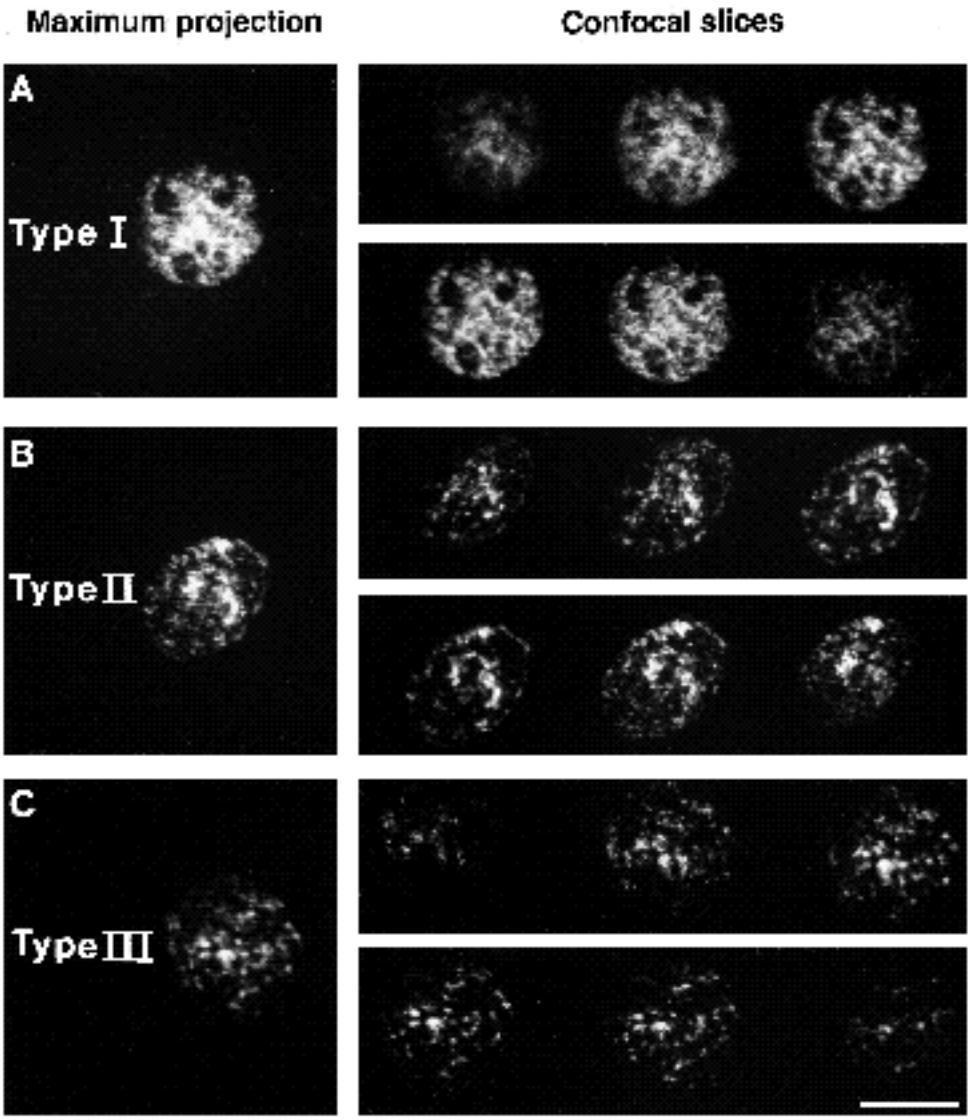

Fig. 7. Foci in unfixed cells viewed using the 'confocal' microscope. Synchronized cells from (A) Type I, early; (B) Type II, mid; and (C) Type III, late S-phase were permeabilized, incubated with 10 μM fluorescein-12-dUTP (60 min) and ~8 optical slices at 0.7 μm intervals taken through typical nuclei; 6 central slices are shown on the right and a maximum projection of all slices on the left. There were 258, 165 and 72 foci/nucleus in (A), (B) and (C), respectively (contiguous foci in adjacent sections in the series were counted as one). Bar, 10 μm.

(Fig. 8E) - a fixative used with extracts of frog's eggs (Mills et al., 1989) - have similar effects. Exposure to the hypotonic conditions often used when nuclei are isolated by conventional procedures diffuses foci so that they become more variable in intensity (Fig. 8G,H). DNase completely removes foci from most cells and residual DNA (visualized by DAPI-staining) appears as a lace-like network (Fig. 8I). Although foci resist digestion with RNase, they become more variable in intensity (Fig. 8J). 0.25 M ammonium sulphate - used to visualize foci in nuclear 'matrices' (Nakayasu and Berezney, 1989), reorganizes DNA and aggregates some foci (Fig. 8K). After fixation with paraformaldehyde, the harsh conditions used for in situ hybridization (without heat denaturation) have little further effect (Fig. 8L); if fixation is omitted, nuclei become sensitive to mechanical damage, but even so, foci are retained (Fig. 8M). Extraction with 0.5% Triton X-100 and 2 M NaCl, a procedure which leaves nascent DNA associated with a nucleoid 'cage' (McCready et al., 1980), also leaves foci, despite complete reorganization of DAPI-staining material (Fig. 8N; note difference in scale).

This study gives the overall impression that the core of each focus contains a stable structure and that different fixation procedures cause the periphery either to disperse or collapse on to the core.

Fluorescent foci resist electroelution

Both polymerase α activity and nascent DNA resist elution even when most chromatin is removed (Jackson and Cook, 1986a,b); therefore we would also expect sites of replication labelled with fluorescein-12-dUTP to resist elution. This proves to be the case. Permeabilized cells were incubated with the analogue for 60 min and treated with nucleases, ~90% of the chromatin was eluted and sites of incorporation were viewed in the fluorescence microscope (Fig. 5). There is, of course, cell to cell variation in the amount of chromatin remaining after elution; again typical examples are illustrated. Sites of incorporation of fluorescein-12-dUTP resist elution (compare Fig. 5F and J; photographs were taken with similar exposures), despite removal of most chromatin (as indicated by faint DAPI staining; compare Fig. 5G and K). Note that now the DAPI staining more

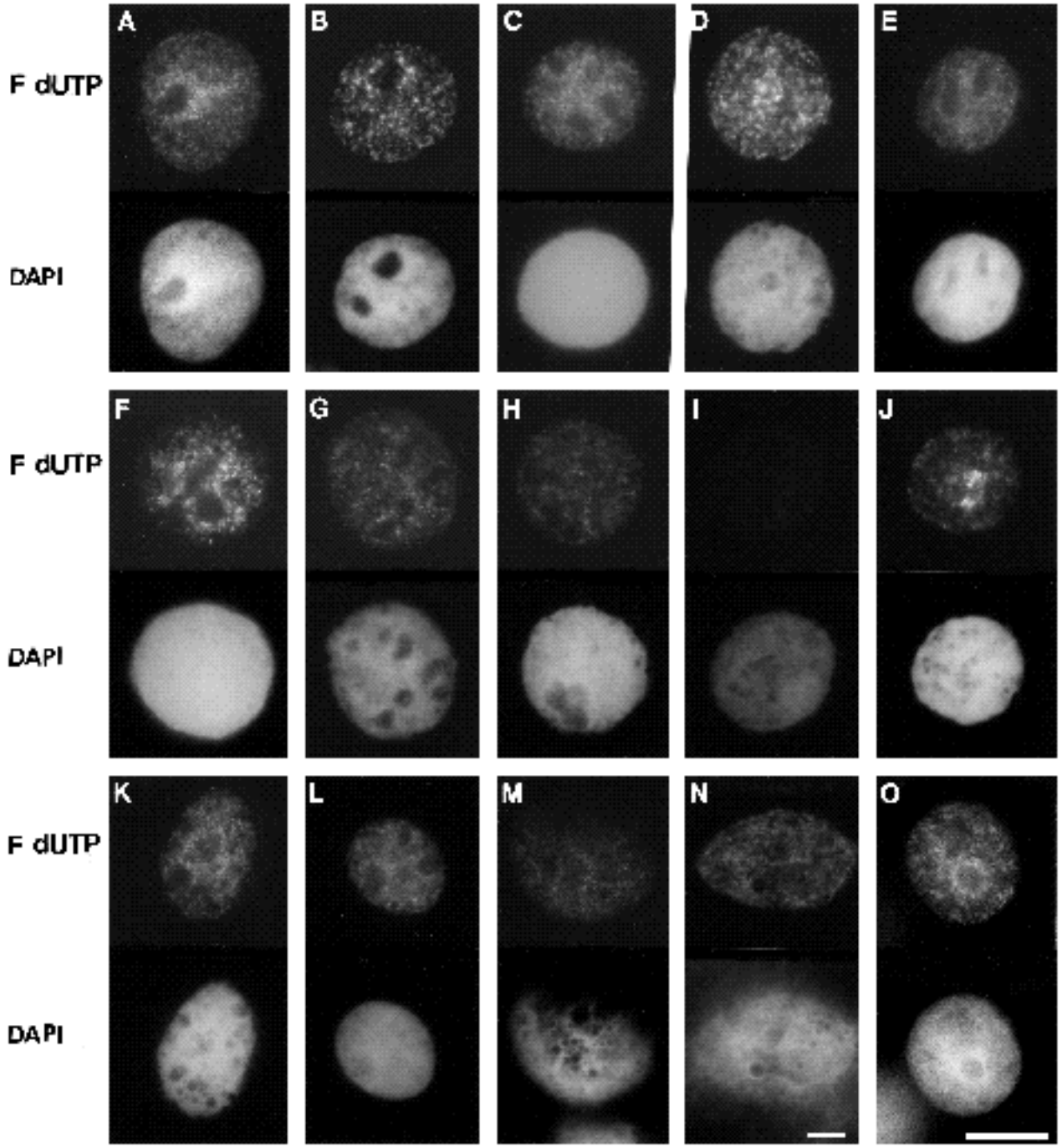

Fig. 8. The effect of fixation on foci. Encapsulated cells were permeabilized with streptolysin O and incubated with 10 μM fluorescein-12-dUTP (F dUTP) for 60 min. Beads were then treated variously (15 min at 4˚C unless stated otherwise) and washed thoroughly in physiological buffer. For each panel, upper half shows cell after incubation with F dUTP; lower half shows same cell after subsequent DAPI staining. All panels are at the same magnification, except for M and N. Bars, 5 μm. (A) 4% paraformaldehyde, pH 7.4. (B) Methanol, −20˚C. (C) 4N HCl. (D) 0.5 mM $CuSO_4$. (E) 10 mM ethylene glycol-bis (succinic acid *N*-hydroxysuccinimide ester), (EGS). (F) 10% trichloroacetic acid. (G) Hypotonic buffer (i.e. PB diluted 10× in distilled water). (H) Hypotonic buffer (i.e. PB diluted 100× in distilled water). (I) 25 u/ml DNase I (35˚C; RNase-free). (J) 5.8 u/ml RNase, (35˚C). (K) 0.25 M $(NH_4)_2SO_4$. (L) Paraformaldehyde fixation (4%) prior to treatment for in situ hybridization (i.e. 50% formamide, 30 mM sodium citrate, 300 mM NaCl). (M) As (L) but without prefixation. (N) 2 M NaCl and 0.5% Triton X-100. (O) Unfixed.

closely mirrors the fluorescence due to incorporated analogue, giving the appearance of a lace-like network. These results mirror those of Nakayasu and Berezney (1989) who showed that foci remained associated with a residual nuclear matrix; here, however, foci are seen in unfixed nuclei.

DISCUSSION

Characterization of DNA synthesis in permeabilized cells

We set out to label sites of replication using conditions that were as close to the physiological as possible. The use of encapsulated cells, a 'physiological' buffer and streptolysin O to permeabilize cell membranes provides a simple and reproducible method to allow access of labelled triphosphates to sites of replication. Fortunately, most replicational activity of the living cell is retained under these conditions; it continues at 40% of the in vivo rate in the presence of 2.5 μM dGTP (Table 2) and higher concentrations give rates equivalent to, or greater than, the in vivo rate (Fig. 4).

We have confirmed previous reports that permeabilizing the nuclear membrane, in our case with Triton X-100, reduces the replication rate (Miller et al., 1978; Jackson et al., 1988), presumably due to the loss of some factor(s). Although lysis with Triton X-100 reduces the rate about four-fold, there is no change in K_m (Fig. 4). Our system gives a non-linear double-reciprocal plot and different K_m values (i.e. 0.9 and 19 μM) depending upon the range of triphosphate concentrations used (Fig. 4B); this may underlie the different K_m values determined previously (Reddy and Pardee, 1982; Krokan et al., 1981; Jackson and Cook, 1986b; Dresler et al., 1988) and stem from differences in leading - and lagging-strand - synthesis. We find no evidence for an intact nuclear membrane buffering polymerization sites from changes in the environment; alterations in pH or Ca^{2+} concentration had comparable effects on streptolysin-O- and Triton-X-100-lysed cells (Fig. 3; Table 1). There is some evidence that the nuclear membrane forms an ionic barrier (e.g. see Williams et al., 1985; Mazzanti et al., 1990) and that deoxynucleotides are 'channelled' or concentrated at replication sites (Reddy and Pardee, 1980; reviewed by Reichard, 1988). A membrane also seems to be required for the initiation of replication in extracts of *Xenopus* eggs and to limit replication to one round per cell cycle (Newport, 1987; Meier et al., 1991; Blow and Laskey, 1988; Leno et al., 1992), but as our system does not initiate our results have little bearing on this problems.

Visualization of 'native' foci in unfixed cells

A variety of analogues (e.g. biotin-11-dUTP, fluorescein-12-dUTP, resorufin-10-dUTP, hydroxycoumarin-6-dUTP) are currently available that permit subsequent visualization of their sites of incorporation by fluorescence microscopy. Although all were incorporated less efficiently than the natural precursor (Table 2), 80-250 discrete sites nevertheless became labelled (Figs 5, 6, 7). Cells at different stages of S-phase had their own typical patterns (Fig. 7) confirming the results of others obtained with fixed material (Nakamura et al., 1986; Nakayasu and Berezney, 1989; Kill et al., 1991).

As our material is unfixed, these results open up the possibility of monitoring the incorporation of fluorescent precursors in real time.

Effect of various fixation procedures on foci

Our ability to visualize foci in unfixed cells allowed us to investigate how fixation affects morphology (Fig. 8). The core of each focus proved to be very stable, although different fixation procedures either dispersed the periphery or collapsed it on to the core. Perhaps not surprisingly, procedures (e.g. methanol, EGS, stabilization with copper sulphate followed by extraction with ammonium sulphate) previously used to visualize foci (Mills et al., 1989; Nakayasu and Berezney, 1989) actually collapsed the foci, making them brighter and more punctate. Fixation with paraformaldehyde was the least disruptive (see also Skaer and Whytock, 1976, 1977).

Replication foci have now been widely visualized by digital microscopy (e.g. see Mills et al., 1989; Fox et al., 1991; Kill et al., 1991; O'Keefe et al., 1992; Humbert et al., 1992). We have used both laser scanning confocal microscopy and digital deconvolution of CCD images to remove out-of-focus flare (Figs 6, 7). The high sensitivity of the CCD camera allows foci to be detected after incubations of only 2.5 and 5 min, when the labile polymerase retains most of its in vivo activity (Fig. 5). The retention of this activity, and the use of physiological conditions, makes it improbable that these focal sites of incorporation are aggregation artifacts. Both these structural and functional criteria make this system an excellent one for studying replication in somatic cells.

Fixed sites of DNA synthesis

These results clearly demonstrate that, even in unfixed material, replication sites are not diffusely spread throughout nuclei but focally concentrated. Assuming that polymerases replicate the ~8 pg DNA in a G_1 nucleus of these aneuploid HeLa cells at ~50 nucleotides/s, ~5500 replication forks must be active at any one time to enable all DNA to be replicated during S-phase; then each focus must contain ~40 forks. Presumably some underlying structure organizes these forks in a focus. Indeed, electron microscopy of nuclei from which ~90% chromatin has been removed (as in Fig. 5J) shows that incorporated biotin is initially associated with discrete ovoid bodies strung along a nucleoskeleton; later, biotin spreads into adjacent chromatin (Hozák et al., 1993). This suggests nascent DNA is extruded from attached replication 'factories' as the template is reeled through the many polymerases in a factory (Cook, 1991).

We thank Dean Jackson for advice and discussion, David Shotton for allowing us to use the confocal microscope, and the Wellcome Trust (ABH) and the Cancer Research Campaign (PRC) for support. Rachel Errington kindly helped with confocal microscopy.

REFERENCES

Ahnert-Higler, G., Mach, W., Fohr, K. J. and Gratzl, M. (1989). Poration by α-toxin and streptolysin O: an approach to analyze intracellular processes. *Meth. Cell Biol.* **31**, 63-90.

Berezney, R. and Coffey, D. S. (1975). Nuclear protein matrix: association with newly synthesized DNA. *Science* **189**, 291-293.

Blow, J. J. and Laskey, R. A. (1986). Initiation of DNA replication in nuclei and purified DNA by a cell-free extract of Xenopus eggs. *Cell* **47**, 577-587.

Blow, J. J. and Laskey, R. A. (1988). A role for the nuclear envelope in controlling DNA replication within the cell cycle. *Nature* **332**, 546-548.

Bravo, R. and Macdonald-Bravo, H. (1987). Existence of two populations of cyclin/proliferating cell nuclear antigen during the cell cycle: association with DNA replication sites. *J. Cell Biol.* **105**, 1549-1554.

Carmo-Fonseca, M., Tollervey, D., Pepperkok, R., Barabino, S. M. L., Meredes, A., Brunner, C., Zamore, P. D., Green, M. R., Hurt, E., and Lamond, A. I. (1991). Mammalian nuclei contain foci which are highly enriched in components of the pre-mRNA splicing machinery. *EMBO J.* **10**, 195-206.

Cook, P. R. (1988). The nucleoskeleton: artefact, passive framework or active site? *J. Cell Sci.* **90**, 1-6.

Cook, P. R. (1991). The nucleoskeleton and the topology of replication. *Cell* **66**, 627-635.

Dolbeare, F. and Gray, J. W. (1988). Use of restriction endonucleases and exonuclease III to expose halogenated pyrimidines for immunochemical staining. *Cytometry* **9**, 631-635.

Dresler, S. L., Frattini, M. G. and Robinson-Hill, R. M. (1988). In situ enzymology of DNA replication and ultraviolet-induced DNA repair synthesis in permeable human cells. *Biochemistry* **27**, 7247-7254.

Finlay, D. R., Newmeyer, D. D., Price, T. M. and Forbes, D. J. (1987). Inhibition of in vitro nuclear transport by a lectin that binds to nuclear pores. *J. Cell Biol.* **104**, 189-200.

Fox, M. H., Arndt-Jovin, D. J., Jovin, T. M., Baumann, P. H. and Robert-Nicoud, M. (1991). Spatial and temporal distribution of DNA replication sites localized by immunofluorescence and confocal microscopy in mouse fibroblasts. *J. Cell Sci.* **99**, 247-253.

Hozák, P., Hassan, A. B., Jackson, D. A. and Cook, P. R. (1993). Visualization of replication factories attached to a nucleoskeleton. *Cell* (in press).

Humbert, C., Santisteban, M. S., Usson, Y., Robert-Nicoud, M. (1992). Intranuclear co-location of newly replicated DNA and PCNA by simultaneous immunofluorescence labelling and confocal microscopy in MCF-7 cells. *J. Cell Sci.* **103**, 97-103.

Hutchison, C. J., Cox, R., Drepaul, R. S., Gomperts, M. and Ford, C. C. (1987). Periodic DNA synthesis in cell free extracts of Xenopus eggs. *EMBO J.* **6**, 2003-2010.

Jackson, D. A. (1990). The organization of replication centres in higher eukaryotes. *BioEssays* **12**, 87-89.

Jackson, D. A. (1991). Structure-function relationships in eukaryotic nuclei. *BioEssays* **13**, 1-10.

Jackson, D. A. and Cook, P. R. (1986a). Replication occurs at a nucleoskeleton. *EMBO J.* **5**, 1403-1410.

Jackson, D. A. and Cook, P. R. (1986b). A cell-cycle dependent DNA polymerase activity that replicates intact DNA in chromatin. *J. Mol. Biol.* **192**, 65-76.

Jackson, D. A. and Cook, P. R. (1986c). Different populations of DNA polymerase α in HeLa cells. *J. Mol. Biol.* **192**, 77-86.

Jackson, D. A., Dickinson, P. and Cook, P. R. (1990). Attachment of DNA to the nucleoskeleton of HeLa cells examined using physiological conditions. *Nucl. Acids Res.* **18**, 4385-4393.

Jackson, D. A., Yuan, J. and Cook, P. R. (1988). A gentle method for preparing cyto- and nucleo-skeletons and associated chromatin. *J. Cell Sci.* **90**, 365-378.

Kill, I. R., Bridger, J. M., Cambell, K. H. S., Maldonado-Codina, G. and Hutchison, C. J. (1991). The timing of the formation and usage of replicase clusters in S-phase nuclei of human diploid fibroblasts. *J. Cell Sci.* **100**, 869-876.

Krokan, H., Wist, E. and Krokan, R. H. (1981). Aphidicolin inhibits DNA synthesis by DNA polymerase α and isolated nuclei by a similar mechanism. *Nucl. Acids Res.* **9**, 4709-4719.

Laskey, R. A., Fairman, M. P. and Blow, J. J. (1989). S-phase of the cell cycle. *Science* **246**, 609-614.

Leno, G. H., Downes, C. S. and Laskey, R. A. (1992). The nuclear membrane prevents replication of human G2 nuclei but not G1 nuclei in Xenopus egg extract. *Cell* **69**, 151-158.

Martelli, A. M., Gilmour, R. R., Falcieri, E., Manzoli, F. A. and Cocco, L. (1990). Temperature dependant association of DNA polymerase activity with the nuclear matrix. *Exp. Cell Res.* **190**, 227-232.

Mazzanti, M., DeFelice, L. J., Cohen, J. and Malter, H. (1990). Ion channels in the nuclear envelope. *Nature* **343**, 764-767.

McCready, S. J., Godwin, J., Mason, D. W., Brazell, I. A. and Cook, P. R. (1980). DNA is replicated at the nuclear cage. *J. Cell Sci.* **46**, 365-386.

Meier, J., Cambell, K. H. S., Ford, C. C., Stick, R. and Hutchison, C. J. (1991). The role of lamin III in nuclear assembly and DNA replication, in cell free extracts of Xenopus eggs. *J. Cell Sci.* **98**, 271-279.

Melan, M. A. and Sluder, G. (1992). Redistribution and differential extraction of soluble proteins in permeabilized cultured cells. *J. Cell Sci.* **101**, 731-743.

Miller, M. R., Castellot, J. J. and Pardee, A. B. (1978). A permeable animal cell preparation for studying macromolecular synthesis: DNA synthesis and the role of deoxyribonucleotides in S phase initiation. *Biochemistry* **17**, 1073-1080.

Mills, A. D., Blow, J. J., White, J. G., Amos, W. B., Wilcock, D. and Laskey, R. A. (1989). Replication occurs at discrete foci spaced throughout nuclei replicating in vitro. *J. Cell Sci.* **94**, 471-477.

Nakamura, H., Morita, T. and Sato, C. (1986). Structural organisation of replicon domains during DNA synthetic phase in the mammalian nucleus. *Exp. Cell Res.* **165**, 291-297.

Nakayasu, H. and Berezney, R. (1989). Mapping replication sites in the eukaryotic cell nucleus. *J. Cell Biol.* **108**, 1-11.

Newport, J. (1987). Nuclear reconstitution in vitro: stages of assembly around protein free DNA. *Cell* **48**, 205-217.

O'Keefe, R. T., Henderson, S. C. and Spector, D. L. (1992). Dynamic organization of DNA replication in mammalian cell nuclei: spatially and temporally defined replication of chromosome-specific α-satellite sequences. *J. Cell Biol.* **116**, 1095-1110.

Pardoll, D. M., Vogelstein, B. and Coffey, D. S. (1980). A fixed site of DNA replication in eukaryotic cells. *Cell* **19**, 527-536.

Reddy, G. P. V. and Pardee, A. B. (1980). Multienzyme complex for metabolic channeling in mammalian DNA replication. *Proc. Nat. Acad. Sci. USA* **77**, 3312-3316.

Reddy, G. P. V. and Pardee, A. B. (1982). Coupled ribonucleoside diphosphate reduction, channelling and incorporation into DNA of mammalian cells. *J. Biol. Chem.* **257**, 12526-12531.

Reichard, P. (1988). Interactions between deoxyribonucleotide and DNA synthesis. *Annu. Rev. Biochem.* **57**, 349-374.

Skaer, R. J. and Whytock, S. (1976). The fixation of nuclei and chromosomes. *J. Cell Sci.* **20**, 221-231.

Skaer, R. J. and Whytock, S. (1977). The fixation of nuclei in glutaraldehyde. *J. Cell Sci.* **27**, 13-21.

Tubo, R. A. and Berezney, R. (1987). Identification of 100 and 150S DNA polymerase alpha-primase megacomplexes solubilized from the nuclear matrix of regenerating rat liver. *J. Biol. Chem.* **262**, 5857-5865.

Williams, D. A., Fogarty, K. E., Tsein, R. Y. and Fay, F. S. (1985). Calcium gradients in single smooth muscle cells revealed by the digital imaging microscope using Fura-2. *Nature* **318**, 558-561.

(Received 22 January 1993 - Accepted 24 February 1993)